Molecular Crystals and Liquid Crystals

ISSN: 1542-1406 (Print) 1563-5287 (Online) Journal homepage: http://www.tandfonline.com/loi/gmcl20

Crystal structures and mesomorphic properties of Schiff base homologs and derivatives, and magnetic properties of their dimeric and dinuclear copper(II) complexes

Norbani Abdullah, Yanti Yana Halid, Tee Jia Ti & Afiq Azil

To cite this article: Norbani Abdullah, Yanti Yana Halid, Tee Jia Ti & Afiq Azil (2016) Crystal structures and mesomorphic properties of Schiff base homologs and derivatives, and magnetic properties of their dimeric and dinuclear copper(II) complexes, Molecular Crystals and Liquid Crystals, 624:1, 132-143, DOI: 10.1080/15421406.2015.1044695

To link to this article: http://dx.doi.org/10.1080/15421406.2015.1044695

MOL. CRYST. LIQ. CRYST.
2016, VOL. 624, NO. 1, 132–143
http://dx.doi.org/10.1080/15421406.2015.1044695

Taylor & Francis
Taylor & Francis Group

Crystal structures and mesomorphic properties of Schiff base homologs and derivatives, and magnetic properties of their dimeric and dinuclear copper(II) complexes

Norbani Abdullah, Yanti Yana Halid, Tee Jia Ti, and Afiq Azil

Department of Chemistry, Faculty of Science, University of Malaya, Kuala Lumpur, Malaysia

ABSTRACT

Three N_2O_4 Schiff. base homologs, H_2L1 (n = 8), H_2L3 ((n = 9), and H_2L4 (n = 10) were obtained from the reactions of 2-HOC_6H_4CHO with $H_2N(CH_2)_{8\text{-}10}NH_2$, while a derivative of H_2L1, namely, H_2L2, was obtained from the reaction of 3,5-X_2-2-HOC_6H_2CHO (X = tert-butyl) with $H_2N(CH_2)_8NH_2$. The Schiff bases H_2L2 (triclinic; P-1), H_2L3 (monoclinic; C2/c), and H_2L4 (monoclinic; P21/c) were single crystals with low melting temperatures (less than 100°C). The homologs exhibited mesomorphisms, while the derivative was not mesomorphic and did not reform crystals from its melt. Copper(II) complexes of H_2L1, H_2L2 and H_2L4 were dimeric, while that of H_2L3 was dinuclear with chelating CH_3COO ligand. These complexes were paramagnetic with insignificant interactions between the copper(II) atoms and have high decomposition temperatures (T_{dec} = 268–304°C). Their melting temperatures (T_{melt} = 138.9–190.2°C) were higher than the corresponding Schiff bases, but they were not mesomorphic.

KEYWORDS

Copper(II) complexes; crystals; magnetism; mesomorphism; Schiff bases

Introduction

Schiff bases formed from polymethylenediamines with suitably selected carbonyls were reported to form metal complexes exhibiting tunable nuclearity, geometry, and magnetic properties [1–11]. As examples, Nathan et al. in 2003 [1] obtained crystals of [Cu(Sal-*n*)] (H_2Sal-*n* were Schiff bases formed from $H_2N(CH_2)_{2\text{-}6}NH_2$ and 2-HOC_6H_4CHO). The structures of these complexes were either dimeric *cis* planar (*n* = 2), monomeric tetrahedral (*n* = 3, 4), or dimeric *trans* planar (*n* = 5, 6). Later in 2009, Mitra et al.[8] reported an almost linear trinuclear Cu(II) complex, $[Cu_3(\mu\text{-L})_2(ClO_4)_2][Cu_3(\mu\text{-L})_2(H_2O)(ClO_4)_2]$ (H_2L was Schiff base formed from 1,3-diaminopentane and 2-HOC_6H_4CHO), which showed strong intratrimer ($J \sim -202\ cm^{-1}$) but very weak intertrimer ($zJ \sim -0.1\ cm^{-1}$) antiferromagnetic interactions. The accumulated knowledge from such works has made it easier to design functional materials with tunable properties.

Our research is focused on thermally stable molecular magnetic materials. The impetus for the work presents in this paper arose from molecular structure of 2,2′-[nonane-1,9-diylbis(nitrilomethylidyne)]diphenol (H_2L3), formed from $H_2N(CH_2)_9NH_2$ and 2-HOC_6H_4CHO [12]. This paper reports the syntheses, characterizations, magnetic,

CONTACT Norbani Abdullah norbania@um.edu.my Norbani Abdullah, Department of Chemistry, Faculty of Science, Universiti of Malaya, 50603 Kuala Lumpur, Malaysia.
Color versions of one or more of the figures in the article can be found online at www.tandfonline.com/gmcl.

thermal, and mesomorphic properties of: (a) two homologs of H_2L3, namely H_2L1 (n = 8) and H_2L4 (n = 10). The molecular structure of H_2L4 was deduced from single-crystal X-ray crystallography; (b) a derivative of H_2L1, labeled as H_2L2, formed as single crystals from $H_2N(CH_2)_8NH_2$ and 3,5-X_2-2-HOC_6H_2CHO (X = *tert*-butyl); and (c) complexes **1**–**4**, formed from the reactions of H_2L1-H_2L3 with $[Cu_2(CH_3COO)_4(H_2O)_2]$, and H_2L4 with $[Cu_2(CH_3(CH_2)_{14}COO)_4]$, respectively. These Schiff bases were of interest since their two N,O-donors were separated by a long and linear alkyl chain (Scheme 1), and hence may form multinuclear and/or ferromagnetic complexes. Accordingly, the main objectives of this work were to study the effect of increasing the carbon chain length and substituent (*tert*-butyl) on the structure, magnetic interaction, thermal stability and mesomorphisms of these compounds. Copper(II) ion was specially selected in this study as it can forms geometrically labile magnetic complexes in order to accommodate the steric dictate of these ligands.

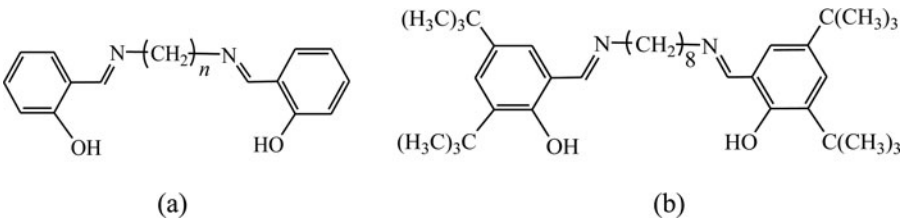

Scheme 1. (a) Structural formulas of: (a) Schiff bases H_2L1 (n = 8) and H_2L4 (n = 10); and (b) H_2L2.

Experimental

Reagents

All chemicals were analar grade and used without further purification.

Physical measurements

^{1}H-NMR spectra were recorded in $CDCl_3$ on a JEOL FT-NMR Lambda 400 MHz spectrometer. Elemental analyses (CHN) were performed on a Perkin-Elmer 2400 Series II elemental analyzer. IR spectra were recorded as KBr discs from 4000–400 cm^{-1} on a Perkin-Elmer RX 1 spectrophotometer. Electronic spectra were recorded on a Shimadzu UV-vis-NIR 3600 spectrometer. Single-crystal X-ray diffraction data were collected at 293(2) K on a Bruker SMART APEX II CCD fitted with Mo$K\alpha$ radiation so that θ_{max} was 27.5°. The data set was corrected for absorption based on multiple scans [13] and reduced using standard methods [14]. The structures were solved by direct methods with SHELXS97 [15] and refined by a full-matrix least-squares procedure on F^2 using SHELXL97 with anisotropic displacement parameters for non-hydrogen atoms and a weighting scheme of the form $w = 1/[\sigma^2(F_o^2) + aP^2 + bP]$, where $P = (F_o^2 + 2F_c^2)/3$). All hydrogen atoms were included in the final refinement in their calculated positions. Magnetic measurements at room temperature were performed on a Sherwood scientific magnetic susceptibility balance, calibrated with $Hg[Co(SCN)_4]$. The diamagnetic corrections were made using Pascal's constants. Temperature dependence of molar susceptibility for **3** was carried out on a Quantum Design MPMS-7 SQUID magnetometer at a constant field of 2000 Oe. Thermogravimetry (TG) was performed in the temperature range of 325–1173 K and scan rate of 20 K min^{-1} on a Perkin-Elmer Pyris Diamond TG/DTA thermal

Table 1. Crystal data and structure refinement for H_2L2 and H_2L4.

Molecule	H_2L2	H_2L4
Chemical formula	$C_{38}H_{60}N_2O_2$	$C_{24}H_{32}N_2O_2$
Formula weight (g mol^{-1})	576.88	761.03
T (K)	293(2)	293(2)
λ (Å)	0.71073	0.71073
Crystal system	Triclinic	Monoclinic
Space group	*P-1*	*P21/c*
a (Å)	8.4479(5)	20.4440(14)
b (Å)	9.7130(7)	5.6277(4)
c (Å)	11.1572(7)	9.1174(6)
α (°)	93.434(5)	90
β (°)	97.544(5)	91.355(6)
γ (°)	100.786(5)	90
V (Å^3)	888.18(10)	1048.69(12)
Z	1	1
D_{calc} (g cm^{-3})	1.079	1.205
Absorption coefficient (mm^{-1})	0.065	0.076
F(000)	318	412
θ range (°)	2.870–25.990	2.990 –25.997
Index ranges	$-10 \le h \le 9$	$-25 \le h \le 24$
	$-11 \le k \le 11$	$-6 \le k \le 6$
	$-13 \le l \le 10$	$-11 \le l \le 11$
Reflections collected	7840	5135
Independent reflections	3496 (0.0325)	2054 (0.0215)
Data/restraints/parameters	3496/0/197	2054/0/129
Goodness-of-fit on F^2	1.031	1.048
Final *R* indices [$I \ge 2.0\sigma(I)$]	$R1 = 0.0863$	$R1 = 0.0375$
	$wR2 = 0.2238$	$wR2 = 0.0936$
	$R1 = 0.1102$,	$R1 = 0.0457$,
R indices (all data)	$wR2 = 0.2464$	$wR2 = 0.0998$
$\Delta\rho_{max}$, $\Delta\rho_{min}$ (e Å^{-3})	1.460, −0.375	0.211, −0.185

instrument under N_2 at a flow rate of 20 cm^3 min^{-1}. Differential scanning calorimetry (DSC) was carried out on a Mettler Toledo DSC 822 instrument in the range 25–150°C under N_2 at a flow rate of 20 cm^3 min^{-1} and scan rate of 10°C min^{-1}. The onset temperatures were quoted for all peaks observed. Polarizing optical microscopy (POM) was carried out on an Olympus polarizing microscope equipped with a Mettler Toledo FP90 central processor and a Linkam THMS 600 hot stage. The heating and cooling rates were 10°C and 1°C min^{-1}, respectively, and the magnification was 50×.

Materials

The synthesis and molecular structure of 2,2'-[nonane-1,9-diylbis(nitrilomethylidyne)] diphenol (H_2L3) were as previously reported [12].

2,2'-[Octane-1,8-diylbis(nitrilomethylidyne)]diphenol (H_2L1)

A mixture of $H_2(NH_2)_8NH_2$ (1.44 g, 10.00 mmol), 2–HOC_6H_4CHO (2.44 g, 20.00 mmol) and a few drops of glacial acetic acid in ethanol (100 cm^3) was refluxed for 1 hr. The yellow powder obtained from the cooled reaction mixture was filtered, washed with ethanol and left to dry at room temperature. Yield 88.5%. Anal. Calc. for $C_{22}H_{28}N_2O_2$: C, 74.97; H, 8.01; N, 7.95; Found: C, 74.95; H, 8.13; N, 8.26. ^{1}H-NMR (400 MHz, $CDCl_3$) δ 13.6 (s, 2H), 8.2 (s, 2H), 7.2 (m, 4H), 6.8 (m, 4H), 3.5 (t, 4H), 1.6 (m, 4H), 1.2 (m, 8H). IR (KBr): ν = 2919, 2849 (C–H aliphatic), 1630 (C=N, imine), 1608 (C=C, aromatic), 1050 (C–O, phenolic) cm^{-1}.

Table 2. Selected bond lengths (Å) and angles (°) for H_2L2 and H_2L4.

Molecule	H_2L2	H_2L4
Bond length		
O(1)-C(1)	1.336(3)	1.3440(14)
O(1)-H(1A)	0.8200	0.8200
N(1)-C(7)	1.254(4)	1.2728(16)
N(1)-C(8)	1.481(4)	1.4575(16)
Angle		
C(1)-O(1)-H(1A)	109.5	109.5
C(7)-N(1)-C(8)	117.6(3)	118.17(11)
O(1)-C(1)-C(6)	122.1(3)	121.49(11)
O(1)-C(1)-C(2)	117.8(2)	118.84(11)
N(1)-C(7)-C(2)	121.4(3)	121.81(12)
N(1)-C(7)-H(7A)	119.3	119.1
N(1)-C(8)-C(9)	110.4(3)	112.05(10)
N(1)-C(8)-H(8A)	109.6	109.2
N(1)-C(8)-H(8B)	109.6	109.2

2,2′-[Octane-1,8-diylbis(nitrilomethylidyne)]-4,4′,6,6′-tetra(tert-butyl)diphenol (H_2L2)

The procedure was the same as H_2L1, replacing 2-HOC_6H_4CHO with 3,5-X_2-2-HOC_6H_2CHO (X = *tert*-butyl). The product was yellow crystals. Yield 90.1%. Anal. Calc. for $C_{38}H_{60}N_2O_2$: C, 79.11; H, 10.48; N, 4.86; Found: C, 79.6; H, 11.1; N, 4.9. ^{1}H-NMR (400 MHz, $CDCl_3$) δ 8.3 (s, 2H), 7.4 (d, 2H), 7.1 (d, 2H), 3.5 (t, 4H), 2.2 (s, 2H), 1.7 (m, 4H), 1.3 (m, 44H).ν = 2959, 2932, 2896, 2860, 2849 (C–H aliphatic), 1634 (C=N, imine), 1594 (C=C, aromatic), 1054 (C–O, phenolic) cm^{-1}.

2,2′-[Decane-1,10-diylbis(nitrilomethylidyne)]diphenol (H_2L4)

The procedure was the same as H_2L1, replacing $H_2(NH_2)_8NH_2$ with $H_2(NH_2)_{10}NH_2$. The product was small yellow crystals. Yield 74.2%. Anal. Calc. for $C_{24}H_{32}N_2O_2$: C, 75.75; H, 8.48; N, 7.36; Found: C, 75.5; H, 8.8; N, 7.3. ^{1}H-NMR (400 MHz, $CDCl_3$) δ 13.6 (s, 2H), 8.3 (s, 2H), 7.3 (d, 2H), 7.2 (t, 2H), 6.9 (d, 2H), 6.8 (t, 2H), 3.5 (t, 4H), 1.7 (m, 4H), 1.2 (m, 12H). IR (KBr): ν = 2929, 2851 (C–H aliphatic), 1632 (C=N imine), 1610 (C=C aromatic), 1048 (C–O, phenolic) cm^{-1}.

[Cu(L1)]$_2$.H$_2$O (1)

An ethanolic solution of H_2L1 (0.71 g, 2.00 mmol,) was added portionwise to a hot ethanolic solution of $[Cu_2(CH_3COO)_4(H_2O)_2]$ (0.81 g, 1.00 mmol). The reaction mixture was refluxed

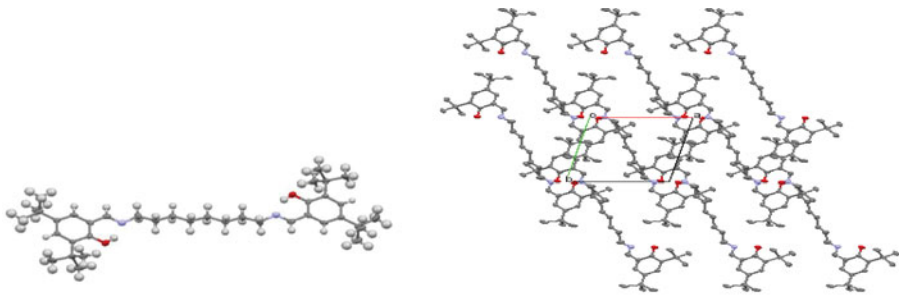

Figure 1. (a) ORTEP view of H_2L2; and (b) its packing diagram viewed along the *c*-axis (H atoms are omitted for clarity).

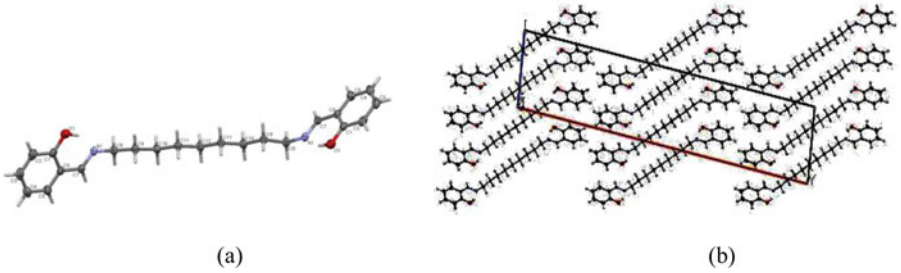

Figure 2. (a) ORTEP view of H_2L3; and (b) its packing diagram viewed along the *c*-axis [12].

for 3 hr, and the khaki-green powder obtained was filtered from the hot reaction mixture and dried in a warm oven (60°C). Yield 82.7%. Anal. Calc. for $C_{44}H_{54}Cu_2N_4O_5$: C, 62.47; H, 6.38; N, 6.62; Found: C, 62.73; H, 6.37; N, 6.66. IR (KBr): $\nu = 3740$ (O-H water), 2915, 2850 (C–H aliphatic), 1619 (C=N imine), 1598 (C=C aromatic), 1145 (C–O, phenolic) cm^{-1}.

[Cu(L2)$_2$].H$_2$O (2)

The procedure was the same as $[Cu(L1)]_2.H_2O$, replacing H_2L1 with H_2L2. The product was a khaki-green powder. Yield 38.8%. Anal. Calc. for $C_{76}H_{118}Cu_2N_4O_5$: C, 70.49; H, 9.20; N, 4.33; Found: C, 70.54; H, 9.69; N, 4.4. IR (KBr): $\nu = 2950, 2928, 2906, 2858$ (C–H aliphatic), 1618 (C=N imine, C=C aromatic), 1169 (C–O, phenolic) cm^{-1}.

[Cu$_2$(L3)(CH$_3$COO)$_2$].2H$_2$O (3)

The procedure was the same as $[Cu(L1)]_2.H_2O$, replacing H_2L1 with H_2L3. The product was a dark brown powder. Yield 32.4%. Anal. Calc. for $C_{27}H_{38}Cu_2N_2O_8$: C, 50.22; H, 5.93; N, 4.34; Found: C, 50.1; H, 6.0; N, 5.0. IR (KBr): $\nu = 3424$ (O-H water), 2922, 2852 (C–H aliphatic), 1624, 1614 (C=N imine, C=C aromatic), 1535 (COO, asym), 1448 (COO, sym) cm^{-1}.

[Cu(L4)]$_2$ (4)

The procedure was the same as $[Cu(L1)]_2.H_2O$, replacing H_2L1 with H_2L4, and $[Cu_2(CH_3COO)_4(H_2O)_2]$ with $[Cu_2(CH_3(CH_2)_{14}COO)_4]$. The product was a khaki-green powder. Yield 67.9%. Anal. Calc. for $C_{48}H_{60}Cu_2N_4O_4$: C, 65.21; H, 6.84; N, 6.34; Found: C, 65.9; H, 7.0; N, 6.2. IR (KBr): $\nu = 2919, 2849$ (C–H aliphatic), 1616 (C=N imine), 1598 (C=C aromatic), 1147 (C–O, phenolic) cm^{-1}.

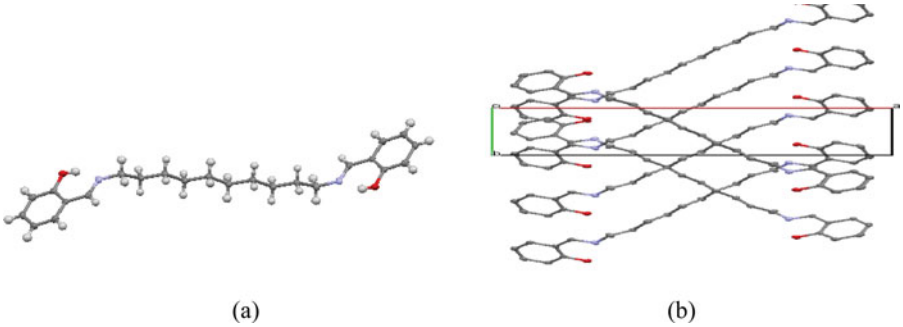

Figure 3. (a) ORTEP view of H_2L4; and (b) its packing diagram, viewed along the *c*-axis (H atoms are omitted for clarity).

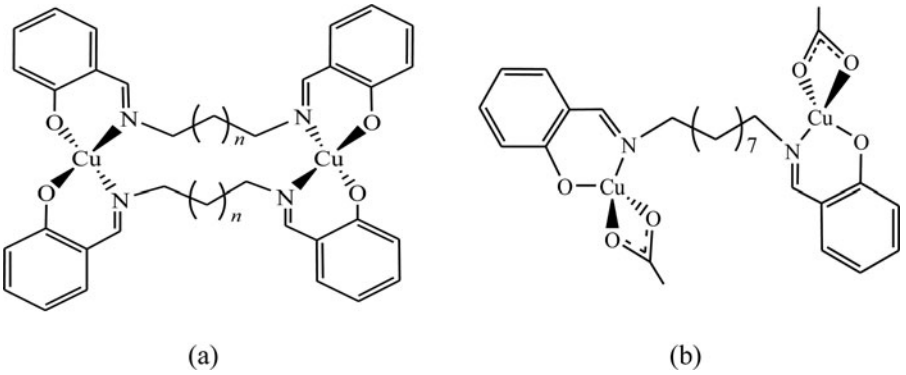

Figure 4. Proposed structural formulas of: (a) 1 ($n = 8$), 4 ($n = 10$); and (b) 3.

Results and discussion

Syntheses and structures of Schiff bases

The Schiff bases H_2L1-H_2L4 were obtained from the condensation reaction of $H_2N(CH_2)_{8\text{-}10}NH_2$ with 2-HOC_6H_4CHO or 3,5-X_2-2-HOC_6H_2CHO (X = *tert*-butyl). H_2L2 ($n = 8$; two *tert*-butyl groups) is a derivative of H_2L1, while H_2L3 and H_2L4 are its homologs. These Schiff bases were crystalline solids. However, H_2L1 ($n = 8$) lost its crystallinity almost immediately once removed from its crystallizing solvents (EtOH-$CHCl_3$). Its structure was deduced from combined instrumental data (Experimental) and by comparison with its derivative, H_2L2 ($n = 8$) and homolog H_2L4 ($n = 10$), which formed stable single crystals. The crystallographic and structure refinement data for both crystals are given in Table 1 and selected bond lengths and angles are given in Table 2. The molecular structures for H_2L2-H_2L4 are shown in Figs. 1–3 (the molecular structure and packing diagram of H_2L3 [12] are reproduced for comparison).

H_2L2 was triclinic, and its space group was *P-1*. The two aromatic rings of each molecule were almost coplanar to each other, while the two OH groups pointed in the opposite direction. There were strong intramolecular N-H-O hydrogen bonding interactions, and the molecules packed so as to optimize the van der Waals interaction between the *tert*-butyl groups at the aromatic rings of neighboring molecules.

The molecular structures and intramolecular N-H-O hydrogen bonding interactions of H_2L3 ($n = 9$) [12] and H_2L4 ($n = 10$) were quite similar to that of H_2L2. However, both molecules were monoclinic, and the space group for H_2L3 was *C*2/*c*, while that for H_2L4 was *P*21/*c*. Finally, the packing of their molecules were quite different. Currently, we are unaware of single crystal structures of homologs and derivatives of these Schiff bases.

Table 3. Hydrogen bonds for H_2L2 and H_2L4 (Å and °).

Molecule	D-H …A	D-H	H …A	D …A	(DHA)
H_2L2	O(1)-H(1A) …N(1)	0.82	1.84	2.5752(14)	148.0
	C(9)-H(9B) …O(1)#2	0.97	2.55	3.3492(15)	139.3
H_2L4	O(1)-H(1A) …N(1)	0.82	1.83	2.572(3)	149.4

Table 4. Analytical data for 1–4.

Complex	λ_{max}/nm (ε_{max}/M^{-1} cm^{-1})	μ_{eff}/BM	T_{dec}/°C
$[Cu(L1)]_2.H_2O$ (**1**)	673 (73)*	2.1	268
$[Cu(L2)]_2.H_2O$ (**2**)	664 (351)#	1.9	280
$[Cu_2(L3)(CH_3COO)_2].2H_2O$ (**3**)	850 (-)	2.6	300
$[Cu(L4)]_2$ (**4**)	600 (260)#	2.0	304
$[Cu(sal\text{-}8)]_2$ [1]	600 nm (-)	1.9	172

*In THF. #In $CHCl_3$. -Solid sample.

Copper(II) complexes of H_2L1-H_2L4

The Schiff bases H_2L1-H_2L3 reacted with $[Cu_2(CH_3COO)_4(H_2O)_2]$ to form $[Cu(L1)]_2.H_2O$ (**1**), $[Cu(L2)]_2.H_2O$ (**2**), and $[Cu_2(L3)(CH_3COO)_2].2H_2O$ (**3**), respectively, while H_2L4 reacted with $[Cu_2(CH_3(CH_2)_{14}COO)_4]$ to form $[Cu(L4)]_2$ (**4**). In these reactions, the dimeric paddle-wheel structure of $[Cu_2(CH_3COO)_4(H_2O)_2]$ and $[Cu_2(CH_3(CH_2)_{14}COO)_4]$ completely dissociated, while the role of carboxylate ion was to deprotonate the Schiff bases, and to act as a chelating ligand for **3** only.

The proposed structural formulas for these complexes (Fig. 4) are based on a combination of several analytical data (Table 4). Hence, **1**, **2**, and **4** were dimeric, similar to $[Cu(Sal\text{-}8)]_2$ ($H_2Sal\text{-}8$ was the Schiff base formed from $H_2N(CH_2)_8NH_2$ and 2-HOC_6H_4CHO [1]), while **3** was dinuclear.

The IR spectral data (Experimental) showed the –C=N peaks at 1630–1635 cm^{-1} for H_2L1-H_2L4, and at 1616-1620 cm^{-1} for their complexes [16]. The shifts to lower energies indicate coordination of the azomethine nitrogen to copper(II) atom in these complexes. Additionally, the spectrum for **3** showed peaks for $\bar{\upsilon}_{as}COO$ at 1535 cm^{-1} and $\bar{\upsilon}_{s}COO$ at 1448 cm^{-1}. The difference (Δ) in the two values was 87 cm^{-1}, indicating a chelating CH_3COO^- ligand [17].

The electronic absorption spectra of **1**, **2**, and **4** showed *d-d* bands at 674, 677, and 600 nm, respectively. These indicate a square pyramidal geometry at Cu(II) [18] for **1** and **2**, and square planar geometry [19,20] for **4**. The spectrum for **3** was recorded for solid sample as it was partially soluble in most solvents. It shows a broad *d-d* band at 850 nm, suggesting a tetrahedral geometry at Cu(II) [21]. The geometrical change for Cu(II) atom in these complexes seems to accord with the molecular structures of their Schiff bases, and reflects an increased flexibility of the alkyl chain, as similarly suggested by Nathan et. al.[1].

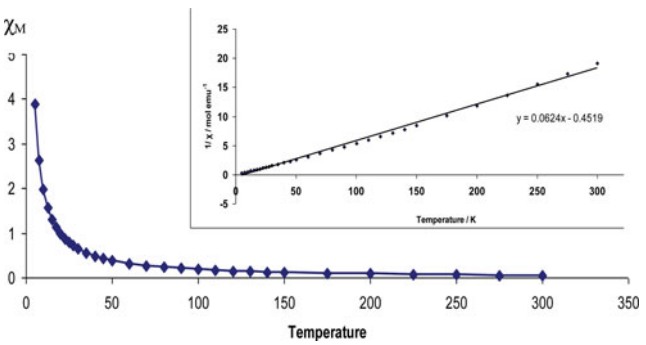

Figure 5. Plot of χ_M vs. *T* for 3.

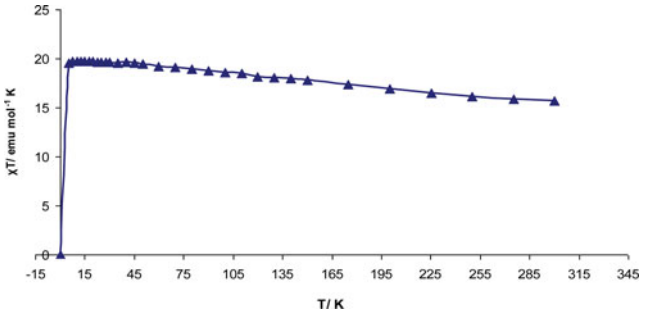

Figure 6. Plot of $\chi_M T$ vs. T for 3.

TG was used to ascertain the purity of complexes **1**–**4**, and to determine their thermal stability. For **1**, there was an initial weight loss of 2.7% at 132°C due to loss of lattice H_2O (calc. 2.1%). The higher temperature at which this occurred suggests that H_2O was H-bonded to the complex. The next weight loss of 76.5% in the temperature range of 268°C–900°C is assigned to loss of $L1^{2-}$ ligand (calc. 82.9%). However, the trace did not plateau out at temperatures above 900°C, suggesting incomplete decomposition of the organic ligand.

For **2**, there was an initial weight loss of 1.1% from 50°C to 280°C due to loss of lattice H_2O (calc. 1.4%). This was followed by a two-step weight loss of 85.9% in the temperature range of 280°C–680°C due to loss of $L2^{2-}$ ligand (calc. 88.8%). The amount of residue above this temperature was 13.0% (calc. 12.4%, assuming pure CuO [22–25]).

For **3**, there was an initial weight loss of 5.0% in the temperature range of 30°C–300°C due to loss of lattice H_2O (calc. 5.6%). The next weight loss occurred in steps of 18.6%, 23.5%, and 28.1% in the temperature range of 300°C–900°C due to loss of CH_3COO^- ion (calc. 18.3%), $H_2N(CH_2)_9NH_2$ molecule (calc. 23.8%), and 2-HOC_6H_4CHO molecule (calc. 27.6%), respectively. The amount of residue above this temperature was 24.8% (calc. 24.6%, assuming pure CuO).

Finally for **4**, there was an initial weight loss of 85.4% in the range of 304°C–850°C due to loss of $L4^{2-}$ ion (calc. 85.6%). The amount of residue above this temperature was 14.4% (calc. 18.0%, assuming pure CuO).

These thermal data support indicate high purities of these complexes, and actually support their proposed structural formulas. The thermal decomposition temperatures were in the range of 268–304°C, and increasing in the following order: **1** < **2** < **3** < **4**. From this, we infer that the thermal stability of these complexes increased with the number of CH_2 group

Table 5. DSC data for H_2L1-H_2L4 and complexes 1–4.

Compound	T (°C)	ΔH (kJ mol^{-1})
H_2L1	75.6	+48.1
H_2L2	89.7	+61.3
H_2L3	61.2	+101.7
H_2L4	57.6	+46.8
$[Cu(L1)]_2.H_2O$ (**1**)	190.2	+41.6
$[Cu(L2)]_2.H_2O$ (**2**)	138.9	+33.9
	183.6	+0.6
$[Cu_2(L3)(CH_3COO)_2].2H_2O$ (**3**)	53.0	+77.7
	102.0	+5.2
$[Cu(L4)]_2$ (**4**)	142.0*	+71.0

*Two overlapping peaks.

in the chain, and for the same number of CH_2, was higher for the ligands with alkyl groups at the aromatic ring.

The room-temperature effective magnetic moments (μ_{eff}) for **1–4** were calculated from the relationship: $\mu_{eff} = [8(\chi_M{}^{corr} - N\alpha)T]^{½}$, where $\chi_M{}^{corr}$ = corrected molar magnetic susceptibility, T = 298 K, and Nα = temperature-independent paramagnetism (60×10^{-6} c.g.s per Cu(II) ion). The μ_{eff} values were 2.1 B.M. for **1**, 1.9 B.M. for **2**, 2.61 B.M. for **3**, and 2.0 B.M. for **4** (the values for **1**, **2**, and **4** were calculated for the monomers). The experimental values for **1**, **2**, and **4** were similar to crystals of [Cu(Sal-8] [1], which was dimeric with *trans*-N_2O_2 donors and distorted planar geometry at Cu(II) in the solid state. Hence, we infer similar structure for **1**, **2**, and **4**. The results also suggest insignificant interaction between the two Cu(II) atoms in the dimers, a consequent of the large separation between them by the alkyl chain.

In contrast, the μ_{eff} value for **3** was higher than the spin-only value expected for a dinuclear complex (2.45 B.M.) [26]. To probe further the magnetic interaction of **3**, its low-temperature magnetic susceptibility was recorded using SQUID magnetometer in the temperature range of 5–300 K. The results, shown as plots of χ_M vs. T and $1/\chi_M$ vs. T in Fig. 5, and as $\chi_M T$ vs. T in Fig. 6, indicate that it deviated from purely paramagnetic behavior as the temperature was lowered, first exhibiting increasing susceptibility with decreasing temperature, and then a sharp decrease below 10 K due to the zero-field effect. Hence, **3** obeyed the Curie-Weiss law (Curie constant, C = 16.03 emu K mol^{-1}; Weiss constant, $\Theta = -7.24$ K). The small negative value for the Weiss constant suggests a weak antiferromagnetic interaction between the two Cu(II) centers, postulated to occur through the lattice H_2O [27,28].

Mesomorphic properties

The phase transitions for H_2L1-H_2L4 and their corresponding complexes were studied by DSC (Table 5), while their optical textures were captured by POM on cooling from the respective isotropic liquid phase (*I*).

The DSC of H_2L1 (Fig. 7(a)) showed an endothermic peak at 75.6°C ($\Delta H = +48.1$ kJ mol^{-1}) for the crystal-to-mesophase transition, and an exothermic peak at 43.9°C ($\Delta H = -40.4$ kJ mol^{-1}) for the mesophase-to-crystal transition. Hence, the liquid strongly supercooled. Its POM showed a smectogenic optical texture at 78.0°C (Fig. 8(a)).

In contrast, its derivative H_2L2 showed an endothermic peak at a higher temperature of 89.7°C ($\Delta H = +61.3$ kJ mol^{-1}) for crystal-to-isotropic liquid transition, but its POM did not show any optical textures.

The DSC of its homolog H_2L3 showed an endothermic peak at a lower temperature of 61.2°C ($\Delta H = +101.7$ kJ mol^{-1}) for assigned to crystal-to-mesophase transition, while its POM showed an optical texture similar to H_2L1 at 52.5°C (Fig. 8(b)).

Finally, the DSC of H_2L4 (Fig. 7(b)) showed an endothermic peak at 57.6°C ($\Delta H = +46.8$ kJ mol^{-1}) for the crystal-to-mesophase transition, and an exothermic peak at 43.9°C ($\Delta H = -40.4$ kJ mol^{-1}) for mesophase-to-crystal transition. Its POM showed an optical texture similar to H_2L1 at 57.0°C (Fig. 8(c)). Hence, these Schiff bases have melting temperatures lower than 100°C; their melting temperatures decreased with increasing alkyl chain length. The homologs H_2L1, H_2L3, and H_2L4 exhibited mesomorphic properties in a narrow temperature range (2–3°C), while the derivative H_2L2 was not mesomorphic. This is a consequent of the unfavorable packing pattern dictated by the two *tert*-butyl groups at the aromatic ring, as indicated from its molecular structure.

For comparison, the DSC scan for complex **1** showed an endothermic peak at 190.2°C ($\Delta H = +41.6$ kJ mol^{-1}, assigned as its melting temperature. For **2**, the scan showed two

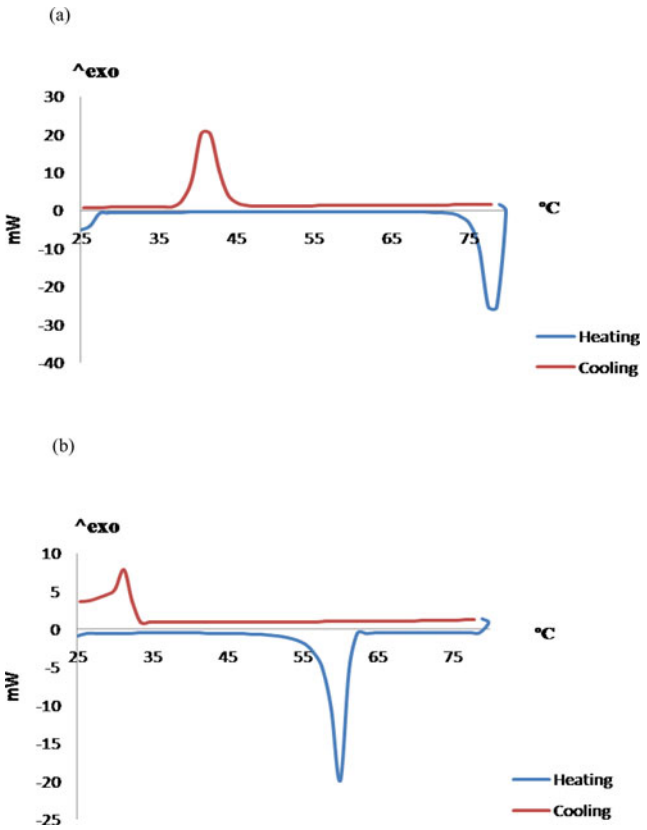

Figure 7. DSC scans for (a) H_2L1; and (b) H_2L4 for one heating-and-cooling cycle.

endothermic peaks at 138.9°C ($\Delta H = +41.6$ kJ mol^{-1}) and 183.6°C ($\Delta H = +0.6$ kJ mol^{-1}), assigned to its melting and clearing temperatures, respectively. Next, the scan for **3** showed two endothermic peaks at 53°C ($\Delta H = +77.7$ kJ mol^{-1}) and 102°C ($\Delta H = +5.2$ kJ mol^{-1}), assigned to the energy required to break the van der Waals forces between L3 ligands and the Cu-OOCCH$_3$ chelating bonds, and to evaporation of lattice H_2O, respectively. Finally for **4**, the scan showed two overlapping endothermic peaks at 142.0°C ($\Delta H_{\text{combined}} = +71.0$ kJ

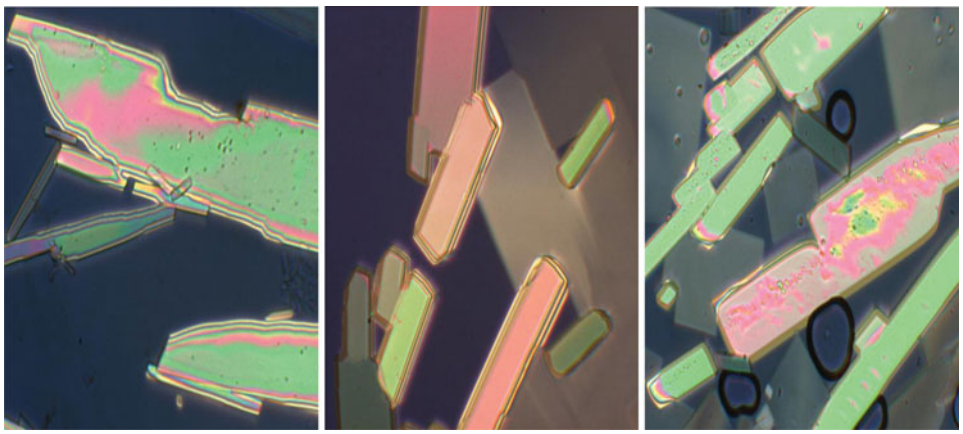

Figure 8. Photomicrographs of: (a) H_2L1 at 77.0°C; (b) H_2L3 at 59.0°C; and (c) H_2L4 at 57.0°C.

mol^{-1}) assigned as its melting and dissociation temperature. However, POM did not show any optical textures for these complexes, and it was noted that the samples remained fluid on cooling from their isotropic temperatures to room temperature. Combining the DSC and POM results, it is suggested that on heating at temperatures above 100°C, the imine bonds of these complexes were hydrolyzed by the lattice H_2O to the corresponding diaminoalkanes and 2-HOC_6H_4CHO (a liquid at 30°C).

Conclusions

In this paper, we presented the syntheses, structures and mesomorphic studies of four N_2O_4-Schiff bases and their corresponding Cu(II) complexes. The Schiff bases were obtained from the reactions of 2-HOC_6H_4CHO with $H_2N(CH_2)_nNH_2$, where $n = 8$ (H_2L1), 9 (H_2L3), 10 (H_2L4), and from the reaction of 3,5-X_2-2-HOC_6H_2CHO (X = *tert*-butyl) with $H_2N(CH_2)_8NH_2$ (H_2L2). H_2L2, H_2L3, and H_2L4 were single crystals. These Schiff bases have melting temperatures lower than 100°C. The homologs (H_2L1, H_2L3, and H_2L4) exhibited mesomorphisms, while the derivative of H_2L1, namely, H_2L2, was not mesomorphic. The copper(II) complexes of H_2L1, H_2L2, and H_2L4 were dimeric, while the complex of H_2L3 was dinuclear with chelating CH_3COO ligand. These complexes were paramagnetic with insignificant interactions between the copper(II) atoms, have high decomposition temperatures, and their melting temperatures were significantly higher than the corresponding Schiff bases. However, they were not mesomorphic.

Supplementary Information

CCDC-1027255 (H_2L2) and 1031111 (H_2L4) contain the supplementary crystallographic data for this paper. These data can be obtained free of charge from the Cambridge Crystallographic Data Centre via www.ccdc.cam.ac.uk/data_request/cif.

Acknowledgments

This research was funded by the Malaysia Ministry of Education for High Impact Research Grant (UM.C/625/1/HIR/MOHE/05) and Fundamental Research Grant Scheme (FP031-2013B), and Universiti Malaya for Postgraduate Research Grants (PV056-2012A and PG023-2013A). We would like to record our thanks to Prof. M. H. Chisholm for the use of research facilities and instruments at the Department of Chemistry, Ohio State University, Columbus, USA.

References

[1] Nathan, L. C., Koehne, J. E., Gilmore, J. M., Hannibal, K. A., Dewhirst, W. E., & Mai, T. D. (2003). *Polyhedron*, *22*, 887.
[2] Kasumov, V. T., & Köksal, F. (2005). *Spectrochim. Acta Mol. Biomol. Spectros*, *61*(1), 225–231.
[3] Abe, K. N. Y., Matsukawa, N., Takashima, H., Iida, M., Tanase, T., Sugibayashi, M., Mukai, H., & Ohta, K. (2006). *Inorg. Chim. Acta*, *359*, 3934.
[4] Bhargavi, G., Rajasekharan, M., & Tuchagues, J.-P. (2009). *Inorg. Chim. Acta*, *362*, 3247.
[5] Maity, D., Chattopadhyay, S., Ghosh, A., Drew, M. G., & Mukhopadhyay, G. (2009). *Polyhedron*, *28*, 812.
[6] Mukherjee, P., Drew, M. G., Tangoulis, V., Estrader, M., Diaz, C., & Ghosh, A. (2009). *Polyhedron*, *28*, 2989.
[7] Chattopadhyay, S., Chakraborty, P., Drew, M. G., & Ghosh, A. (2009). *Inorg. Chim. Acta*, *362*, 502.

[8] Ray, A., Sadhukhan, D., Rosair, G. M., Gómez-García, C. J., & Mitra, S. (2009), *Polyhedron*, *28*, 3542.
[9] Naiya, S., Drew, M. G., Estarellas, C., Frontera, A., & Ghosh, A. (2010). *Inorg. Chim. Acta*, *363*, 3904.
[10] Biswas, A., Drew, M. G., & Ghosh, A. (2010). *Polyhedron*, *29*, 1029.
[11] Mukherjee, P., Kar, P., Ianelli, S., & Ghosh, A. (2011). *Inorg. Chim. Acta*, *365*, 318.
[12] Abdullah, N., Lo, K. M., Tajuddin, H. A., Tee, J. T., & Ng, S. W. (2008). *Acta Crystallogr. Sect. E.-Struct Rep. Online*, *64(12)*, 2494.
[13] Sheldrick, G. M. (1997). *SHELX Program for Crystal Structure Solution and Refinement*, University of Göttingen, Germany.
[14] APEX2 & SAINT Bruker (2007). *AXS Inc Madison*, Wisconsin, USA.
[15] Sheldrick, G. M. (2007). *Acta Crystallogr. Sect. A*, *64*(1), 112.
[16] Prabhuswamy, M., Dinesha, Pampa,K. J., Kumar, S. M., Nagaraja, G. K., & Lokanath, N. K. (2014). *Mol. Cryst. Liq. Cryst*. *593*(1), 243–252.
[17] Deacon, G., & Phillips, R. (1980). *Coord. Chem. Rev.*, *33*, 227.
[18] Kato, M. B. Jonassen, H. B., & Fanning, J. C. (1964). *Chem. Rev*., *64*, 99.
[19] Aazam, E., El Husseiny, A., & Al-Amri, H. (2012). *Arabian J. Chem.*, *5*, 45.
[20] Vanco, J., Marek, J., Travnicek, Z., Racanska, E., Muselik, J., & Svajlenova, O. (2008). *J. Inorg. Biochem.*, *102*, 595.
[21] Bhatt, V. D., & Ram, S. R. (2012). *Chem. Sci.*, *3*, 1.
[22] Ferenc, W., Walków-Dziewulska, A., & Sadowski, P. (2005). *J. Therm. Anal. Calorim.*, *82*, 365.
[23] Turek, A., Kobylecka J., & Ptaszynski, B. (2005). *J. Therm. Anal. Calorim.*, *78*(2), 513.
[24] Wang, F. Q., Weng, D. F., Zheng, X. J., Zhang, J. J., Mad, H., & Jin, L. P. (2007). *Inorg. Chim. Acta*, *360*, 2029.
[25] Arshad, M., Rehman, S., Khan, S. A., Masud, K., Arshad, N., & Ghani, A. (2000). *Thermochim. Acta*, 143.
[26] Khan, O. (1996). *Curr. Opin. Solid State Mater. Sci.*, *1*, 547.
[27] Zhao, P. S., Guo, Z. Y., Sui, J., Wang, J., & Jian, F. *Bull. Korean Chem. Soc.*, *32*, 1.
[28] Bleaney, B., & Bowers, K. (1952). *Proc. R. Soc. London, Ser. A*, *214*, 451.